Paper No.
05267

CORROSION2005

REAL-TIME MONITORING OF CORROSION IN CONCRETE UTILIZING COUPLED MULTIELECTRODE ARRAY SENSORS

Xiaodong Sun
Corr Instruments, LLC
San Antonio TX, USA

ABSTRACT

Real-time corrosion monitoring of carbon steel rebar materials in concrete was conducted utilizing coupled multielectrode sensors. It was demonstrated that the coupled multielectrode sensor is a quantitative and real-time tool for the monitoring localized corrosion rates in concrete. The coupled multielectrode sensor also provided real-time indications for the effectiveness of cathodic protection in concrete.

Keywords: Corrosion monitoring, corrosion in concrete, corrosion sensor, localized corrosion, online corrosion sensor, real-time corrosion sensor, multielectrode sensor, coupled multiple electrodes, cathodic protection.

INTRODUCTION

Steel reinforcements in concrete structures exposed to aggressive conditions, such as marine environments and de-icing salts, are subject to corrosion degradation and significant reductions in their service lives. To mitigate corrosion prior to significant degradation and optimize the performance of such concrete structures, various sensors have been used to detect the corrosion and to provide early warning [1-5]. Coupled multielectrode sensors were developed on the basis of a new technology and have been recently used as *in situ* and online monitors for non-uniform corrosion—especially localized corrosion—in laboratories and industry applications[6-11]. They have also been used to give quantitative real-time corrosion signals for cathodically protected systems[12] and coated metal components[13], and as a real-time monitor for the corrosion of carbon steel materials in soil with or without cathodic protections[14]. In this study, coupled multielectrode corrosion sensors were used to measure the real-time corrosion rate of rebar materials in concrete. The experimentally measured corrosion rates in different conditions, including cathodic protection conditions are also presented.

EXPERIMENTAL PROCEDURES

A nanoCorr™* A–50 coupled multielectrode analyzer,[12-15] manufactured by Corr Instruments (San Antonio, TX, USA), was used in the experiment (*Figure 1*). *Figure 2* shows the principle of the analyzer. The analyzer couples the multiple sensing electrodes made of the same material as that used in a given application to a common joint through resistors. In a non-uniform corrosion condition, some of the electrodes corrode in preference to others and therefore a dispersion in the measured currents from sensing electrodes is observed. Thus, the multiple electrodes in the probe simulate a single piece of metal[6-8]. If the sensing elements are sufficiently small so that separation of anodic and cathodic reactions between different electrodes can be assumed, the localized corrosion rates can be obtained directly from the measured current densities, which correspond to non-uniform corrosion. The coupled multielectrode corrosion analyzer shown in *Figure 1* has a high current resolution (10^{-12} A) and allows the measurement of coupling currents for up to 50 electrodes. *Figure 3* shows that three probes were connected to the coupled multielectrode analyzer and measured at same time.

Figure 3 shows coupled multielectrode probes used in this study. Their sensing electrodes were made from carbon steel concrete rebar wire (1.5 mm in diameter and 1.77 mm^2 in electrode surface area). Each probe had 16 electrodes flush-mounted in epoxy. Prior to the test, the surfaces of the sensing electrodes for each multielectrode probe were polished to 600 grit and rinsed first with distilled water and then with acetone.

Figure 4 shows the experimental setup during the partial immersion tests. The probes and sacrificial aluminum anodes were vertically buried into a commercial grade concrete-sand mixture (Mason Mix NO. 1136) by Quikrete Companies (Atlanta, GA, USA), which was initially mixed with distilled water. The concrete was formed in a plastic container with a dimension of 37 cm (length) x 25 cm (width) x16 cm (height) and cured while it was submerged in distilled water. Corrosion rate measurements were taken shortly before the probes were buried into the concrete and then continued for approximately seven days, while the concrete was continuously submerged in the distilled water. On the seventh day, the concrete was removed from the plastic container and partially immersed in a shallow bath filled with simulated seawater (3%wt sea salt by Vigo Importing Co., Tampa, Florida, USA), to allow the chloride to diffuse from the bottom and sides of the concrete to the sensing surface of the coupled multielectrode probes, and to see the response of the probe to the arrival of chloride. Because of evaporation, frequent additions of simulated seawater were made to the bath to ensure that the bottom section of the concrete was always immersed in 2 to 3 cm of the simulated seawater. Because of evaporation and the addition of simulated seawater, the salt concentration was probably higher than 3%wt at the end of the testing period. A large amount of the salts were crystallized on the side surfaces of the concrete. The exact concentration in the bath at the end of the test could not be determined. The sensing surfaces of Probe 1 (right in *Figure 4*) and Probe 2 (left in *Figure 4*) were approximately 1.48 cm and 2.65 cm from the bottom surface of the concrete, and both probes were 8 cm from side surfaces (left or right) of the concrete. Therefore, the diffusion paths for chloride to reach the sensing surfaces of Probe 1 and Probe 2 are approximately 1.48 cm and 2.65 cm, respectively.

Another experiment was conducted for corrosion rate measurement under cathodic protection conditions. *Figure 5* shows the wiring configuration between the multielectrode probes, the reference electrode, and the sacrificial anodes. The common joint of the corrosion analyzer is shown in *Figure 1*. The sacrificial anodes were the aluminum wires vertically buried near the probes. A saturated calomel

* nanoCorr and CorrVisual are trademarks of Corr Instruments, LLC.

electrode (SCE) was dipped into the concrete near the probes and used as the reference electrode for electrochemical potential measurements.

A notebook computer and factory-supplied software, CorrVisual™*, were used in conjunction with the multielectrode analyzer. The current from each electrode of the probes, the electrochemical potential of each probe, and the temperature were logged at predetermined time intervals (usually 20 to 600 seconds) and saved in a computer file. Processed signals—such as the localized corrosion current, the cumulative charge for each sensor, and the corrosion rate and cumulative corrosion damage (or penetration depth) for each probe—were also saved into separate files. During the measurement, the directly measured currents and the processed results—such as the minimum current, maximum current, mean current, current densities, corrosion rates, cumulative charges, penetration depth, and electrochemical potential—were also dynamically displayed on the computer screen, in both numerical and graphical forms.

The coupled multielectrode probes and corrosion analyzer used in these studies were tested in a distilled water, in a simulated 3%wt of sea salt water (as used in this study), and in a solution of 3%wt sea salt plus 10 mM H_2O_2 at room temperature, and the results were reported in a previous publication [12] (*Figure 6*).

RESULTS AND DISCUSSIONS

Corrosion Rate in Concrete Submerged in Distilled Water and During Initial Mixing

Figure 7 shows the corrosion rates of rebar material measured from two independent coupled multielectrode array probes in concrete. The concrete was mixed with distilled water and then submerged in distilled water during the test. The non-uniform corrosion rates in air (localized corrosion rate) were at or below the specified lower detection limit of the coupled multielectrode analyzer (10 nm/year). Upon placing the probes into the freshly mixed concrete (with distilled water), the corrosion rate from the two probes instantaneously increased to approximately 70 µm /year, which is between the corrosion rates of the carbon steel material in simulated seawater and in distilled water (see *Figure 6*). The corrosion rate of Probe 1 stayed at about 70 µm/year for about 10 hours and then started to decrease. The corrosion rate of Probe 2 started to decrease approximately two hours after the initial increase. In 17 hours, the corrosion rates from both probes decreased to 5µm/year. After the first 17 hours, the corrosion rates from the two probes gradually decreased, reaching close to 3 µm/year in the seventh day. This decrease in corrosion rate is understandable because the concrete generates an alkaline environment which helps passivate the steel in the presence of distilled water.

Figure 8 shows the non-uniform corrosion penetration depths calculated by the software and by using the published procedures[7] according to the measured corrosion rate as shown in *Figure 7*. Most of the penetration caused by the non-uniform corrosion took place in the first day after the probes were buried in the concrete, which was initially mixed with and subsequently submerged in distilled water.

Compared with the corrosion rate of the same carbon steel material in soil soaked with either distilled water or simulated seawater[14], the initial corrosion rate measured in the concrete was higher and lasted longer than that measured in the densely packed soil. This is most likely an indication that the mass-transport of the corrosion products from and the migration of corrosion reactants to the electrode surfaces at the beginning of the test (before the concrete was set) were faster than those in the densely packed soil. After the concrete was set, however, the corrosion rate in the concrete was as low as that observed in the densely packed soil[14].

Responses of Corrosion Rate to Immersion in Simulated Seawater

Figure 9 shows the non-uniform corrosion rate measured from the probe whose sensing surface was 1.48 cm from the concrete bottom surface contacting the simulated seawater. There was an increase in corrosion rate approximately two days after the immersion of the concrete into the simulated seawater. This increase was most likely caused by the arrival of chloride to the surface of the probe through diffusion. After the increase, two days following the immersion in simulated seawater, the corrosion rate gradually decreased, reaching 0.5 µm/year at the end of the testing period (a 32-day duration).

Figure 10 shows the non-uniform corrosion rate measured from the probe whose sensing surface was 2.65 cm from the concrete bottom surface contacting simulated seawater. Unlike the results shown in *Figure 9*, there was not a significant increase in the corrosion rate after the immersion of the concrete into simulated seawater. It is unclear whether the slight increase four days after immersion or the gradual increase seven days after the immersion was due to the arrival of chloride to the probe sensing surface. The steady-state corrosion rate at the end of the 37-day test was 2.4 µm/year. This is close to the value measured by the first probe (*Figure 9*).

Corrosion Rate Increase Immediately After Decoupling

During the testing period, the probe was disconnected from the corrosion analyzer several times, and the electrodes in the probes were decoupled (each electrode was left in open-circuit condition). The corrosion rate from each probe was significantly higher immediately after the probe was reconnected and the electrodes were recoupled to resume the measurements. This behavior is illustrated in *Figure 11*. The increase observed when the probe was recoupled is attributed to the mass-transfer effect. At the time the electrodes were decoupled, there was no continued flow of electrons from the anodic electrodes to the cathodic electrodes. The corrosion products produced during the coupling had more time to diffuse from corroded sites and the reactants had more time to diffuse to the cathodic sites. At the time the probe was reconnected and the electrodes in the probe were recoupled, the electron flows resumed. The relatively high concentrations of reactants and low concentrations of corrosion products near the electrodes, at the end of decoupling, led to a high corrosion rate at the instant the electrodes were recoupled. Because of the mass-transfer limit, the corrosion rate decreased rapidly, and reached a steady-state value that was the same as the value prior to the decoupling. *Figure 12* shows both the probe potentials and the corrosion rates before and after the decoupling. It appeared that the measured potentials of the two probes immediately after the recoupling was slightly lower than the corresponding values prior to the decoupling and gradually increased to the previous values. The lower corrosion potential suggests that the higher corrosion rates measured immediately after the re-coupling were probably due to the lower concentration of the corrosion products, rather than the higher concentration of the oxidant (e.g., oxygen) at the electrode surface.

Corrosion Rate Under Cathodic Protection Conditions

The multielectrode probes in the concrete partially immersed in simulated seawater were connected to the aluminum sacrificial anodes (*Figure 4*), to measure the corrosion rate under cathodic protection conditions. *Figure 13* shows the measured corrosion rates of the carbon steel multielectrode probes and the electrochemical potentials of the coupling joint of Probe 1 before, during, and after the

cathodic protection. As soon as the carbon steel electrodes were connected to the aluminum electrodes and cathodically protected, the electrochemical potential of Probe 1 decreased from -0.735 V(SCE) to -1.27 V(SCE), and the corrosion rates of both probes dropped to 1.3 nm/year, which is below the lower detection limit of the corrosion analyzer (10 nm/year), suggesting that the carbon steel material in the two probes was adequately protected. When the cathodic protection was removed, the potential returned to -1.0 V(SCE), which is significantly lower than the previous value. However, the corrosion rates from both of the probes were significantly higher than those of the previous value. The lower potential and the higher corrosion rate immediately after removing the cathodic protection suggest that the concentrations were low for the corrosion products and/or high for the reactants such as oxygen during the cathodic protection.

CONCLUSION

A coupled multielectrode sensor probe was successfully used to measure the real-time corrosion rate of concrete rebar material in concrete in a laboratory. The steady-state corrosion rates measured in the concrete partially immersion in simulated seawater were 0.5 to 2.4 µm/year. When the carbon steel electrodes of the probe were connected to sacrificial aluminum anodes, the corrosion rate decreased instantaneously to a value that is below the lower detection limit of the instruments (10 nm/year), suggesting that the coupled multielectrode array sensor can be used as a real-time tool to measure the effectiveness of cathodic protection for steel reinforcements in concrete.

ACKNOWLEDGMENTS

The author acknowledge narasi sridhar and Lietai Yang for their technical discussions, useful suggestions and valuable comments.

REFERENCES

1. P. Schiessl, M. Raupach, "Monitoring System for Corrosion Risk for Steel in Concrete," Concrete International N0. 7, 1992, pp. 52-55.

2. P. Schiessl, M. Raupach, "New Approach for Monitoring of the Corrosion Risk for the Reinforcement-Installation of Sensors," Proceedings of International Conference: Concrete Across Borders, Odense, Denmark, June, 1994, pp. 65-78.

3. B. Espelid, K., Videm, I. Markey, "Strategies for Monitoring Durability of Concrete Structure," Proceedings of International Conference: Repair of Concrete Structures, Svolvar, Norway, May 1997, pp. 233-242.

4. R. Bassler, J. Mietz, M. Raupach, and O. Klinghoffer, "Corrosion Monitoring Sensors for Durability Assessment of Concrete Structures," in Smart Structures and Materials 200.0. Smart Systems for Bridges, Structures, and Highways, Proceedings of SPIEs —The International Society for Optical Engineering, Vol. 3988, page 32-39 (2000).

5. H. Takeda, A. Gokce, K.-I. Horiguchi and T. Maruya, "Quantitative Estimation about Macro Cell Corrosion of Concrete Structures Damaged by Salt Contamination," Taisei Kensetsu Gijutsu Sentaho, 35 (2002), pp. 54-60.

6. L. Yang and N. Sridhar, *Monitoring of Localized Corrosion,* ASM Handbook, Volume 13A, "Corrosion: Fundamentals, Testing, and Protection," Stephen. D. Crammer and Bernard S. Covino, Jr. Eds, ASM International, Materials Park, Ohio, 2003, pp. 519-524.

7. L. Yang, N. Sridhar, O. Pensado, and D.S. Dunn, *Corrosion*, 58 (2002), p.1004.

8. L. Yang and N. Sridhar, "Coupled Multielectrode Online Corrosion Sensor Materials Performance," 42(9), pp. 48-52 (2003).

9. M. H. Dorsey, L. Yang and N. Sridhar, "Cooling Water Monitoring Using Coupled Multielectrode Array Sensors and Other On-line Tools," CORROSION/2004, paper no. 04077, (Houston, TX: NACE International, 2004).

10. L. Yang, R.T. Pabalan, L. Browning, and G.C. Cragnolino, "Measurement of Corrosion in Saturated Solutions under Salt Deposits Using Coupled Multielectrode Array Sensors," CORROSION/2003, paper no. 426 (Houston, TX: NACE, 2003).

11. C.S. Brossia and L. Yang, "Studies of Microbiologically Induced Corrosion Using a Coupled Multielectrode Array Sensor," CORROSION/2003, paper no. 575 (Houston, TX: NACE, 2003).

12. X. Sun, Xiaodong Sun, "Online Monitoring of Corrosion under Cathodic Protection Conditions Utilizing Coupled Multielectrode Sensors," CORROSION/2004, paper no. 04094, (Houston, TX: NACE International, 2004).

13. X. Sun, “Online Monitoring of Undercoating Corrosions Utilizing Coupled Multielectrode Sensors,” CORROSION/2004, paper no.04033 (Houston, TX: NACE, 2004).

14. X. Sun, “Real-time Corrosion Monitoring in Soil with Coupled Multielectrode Sensors,” CORROSION/2005, paper no.05381 (Houston, TX: NACE, 2005).

15. S. Moreno, “Corrosion Analyzer,” Materials Performance, 43(4), (2004) p.15.

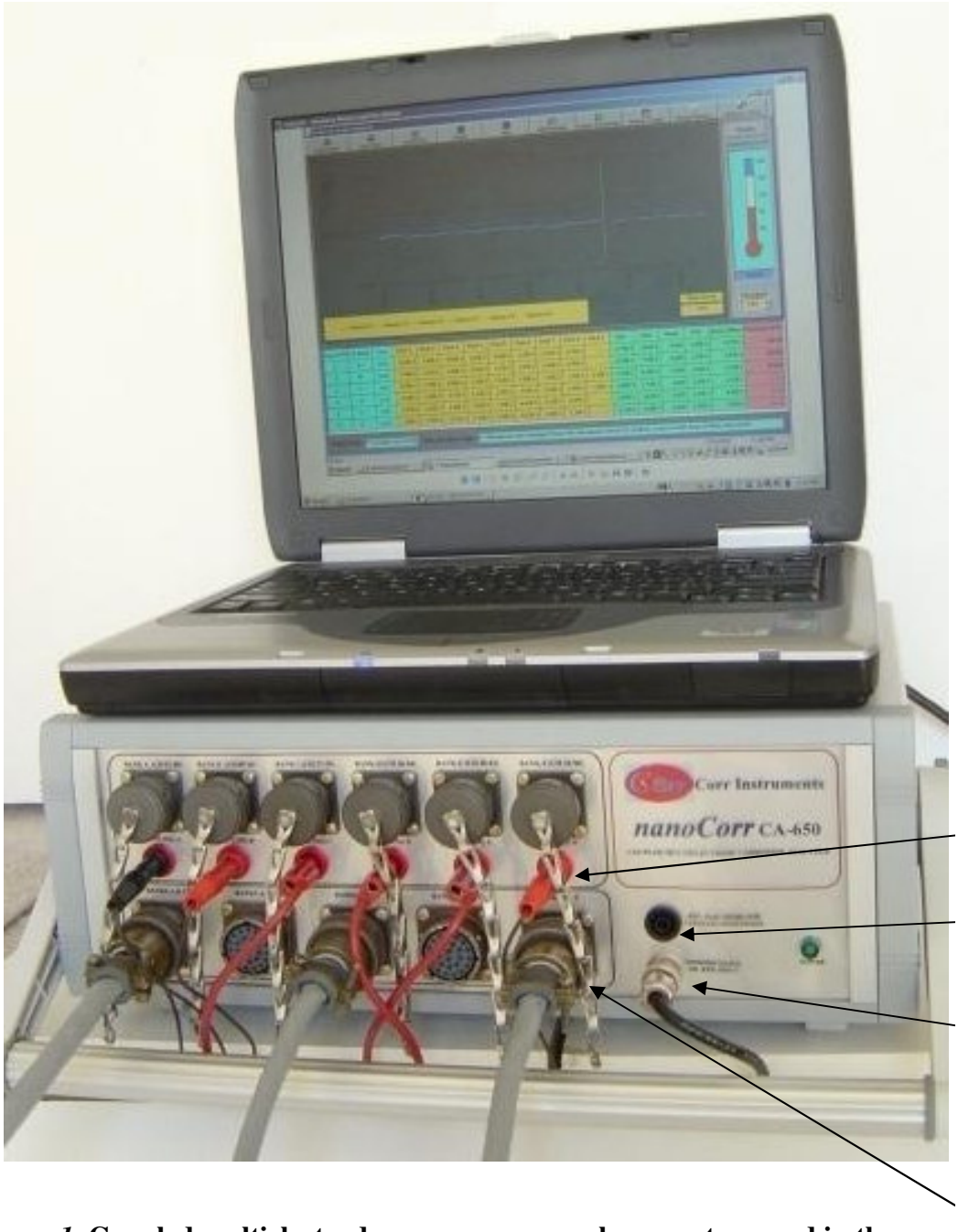

Figure 1. **Coupled multielectrode array sensor analyzer system used in the experiment. As shown in the picture, the analyzer was used to measure the corrosion rates and corrosion potentials simultaneously for three independent 16-electrode probes.**

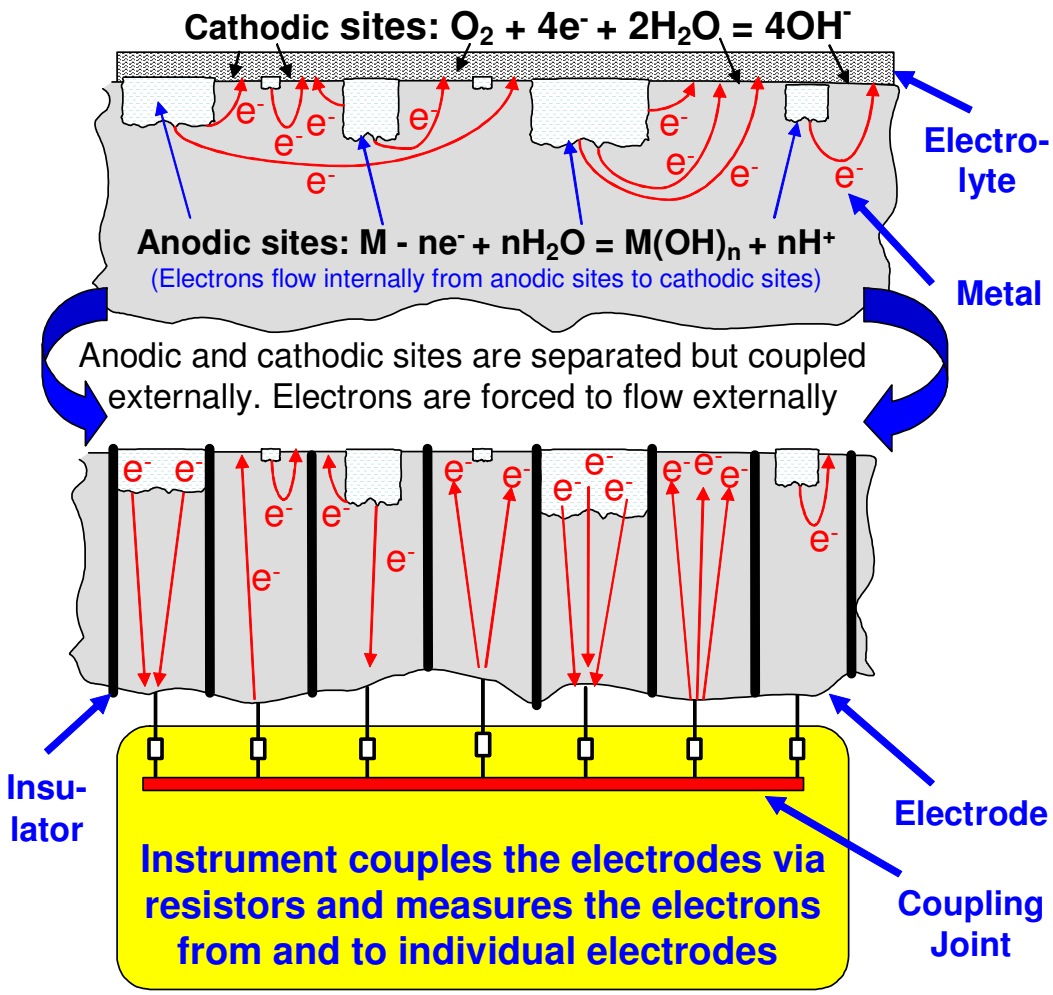

Figure 2. **Schematic diagram showing the principle of the coupled multielectrode array sensor analyzer used in the experiment.**

Figure 3. **Coupled multielectrode array sensor probes used in the experiment.**

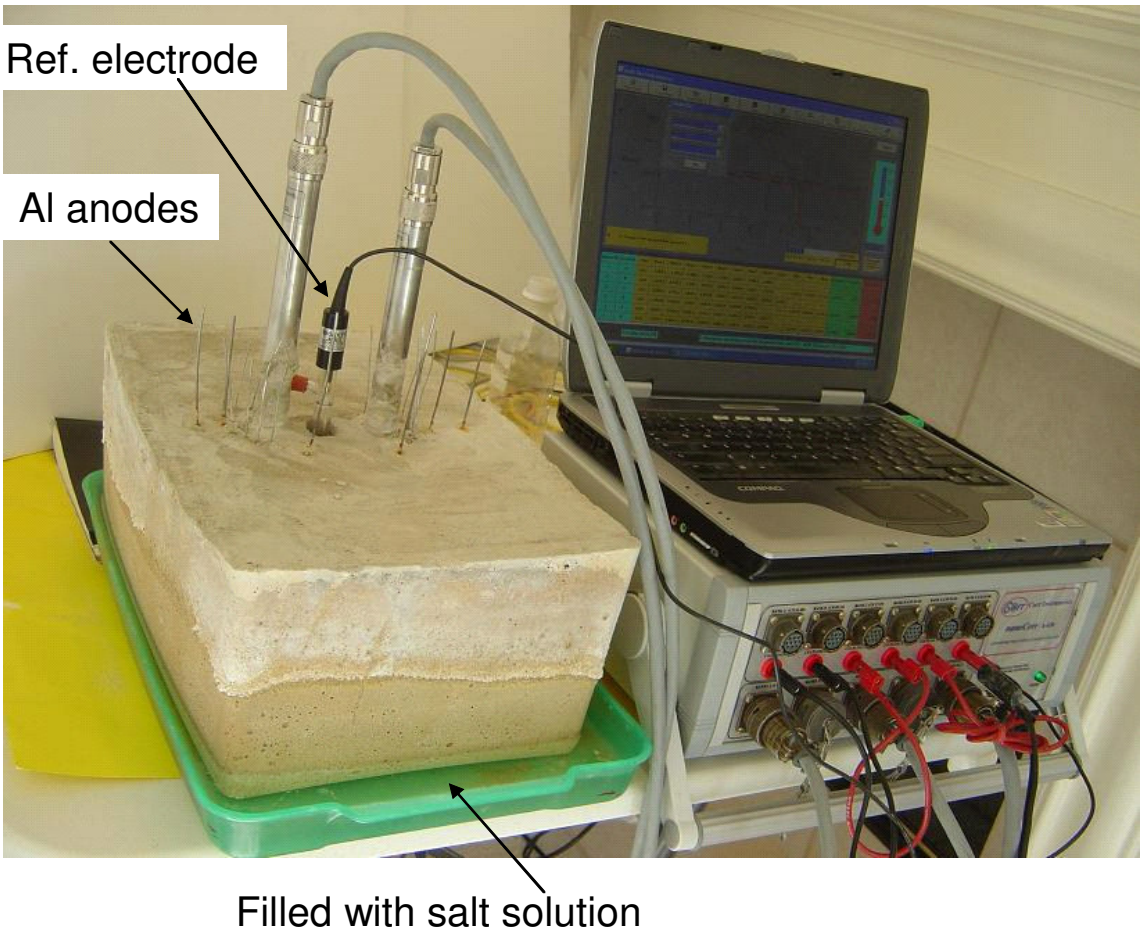

Figure 4. **Typical experimental setup during partial immersion in simulated seawater.**

Note: **The sensing surfaces of Probe 1 (right) and Probe 2 (left) were 1.48 cm and 2.65 cm, respectively, from the bottom surface of the concrete. The Al anodes were used for cathodic protection during the test.**

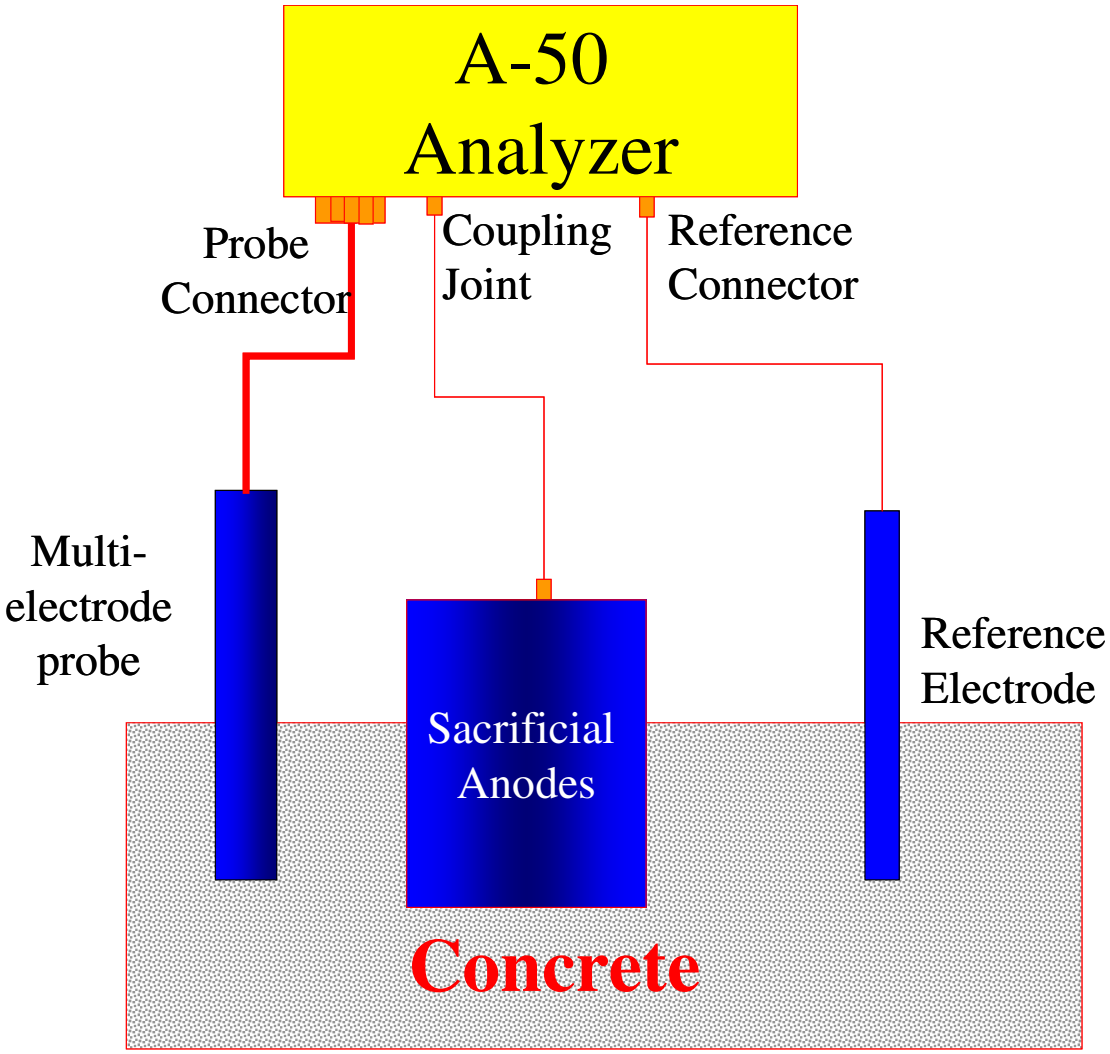

Figure 5. **Schematic diagram showing the wiring configuration during the cathodic protection test.**

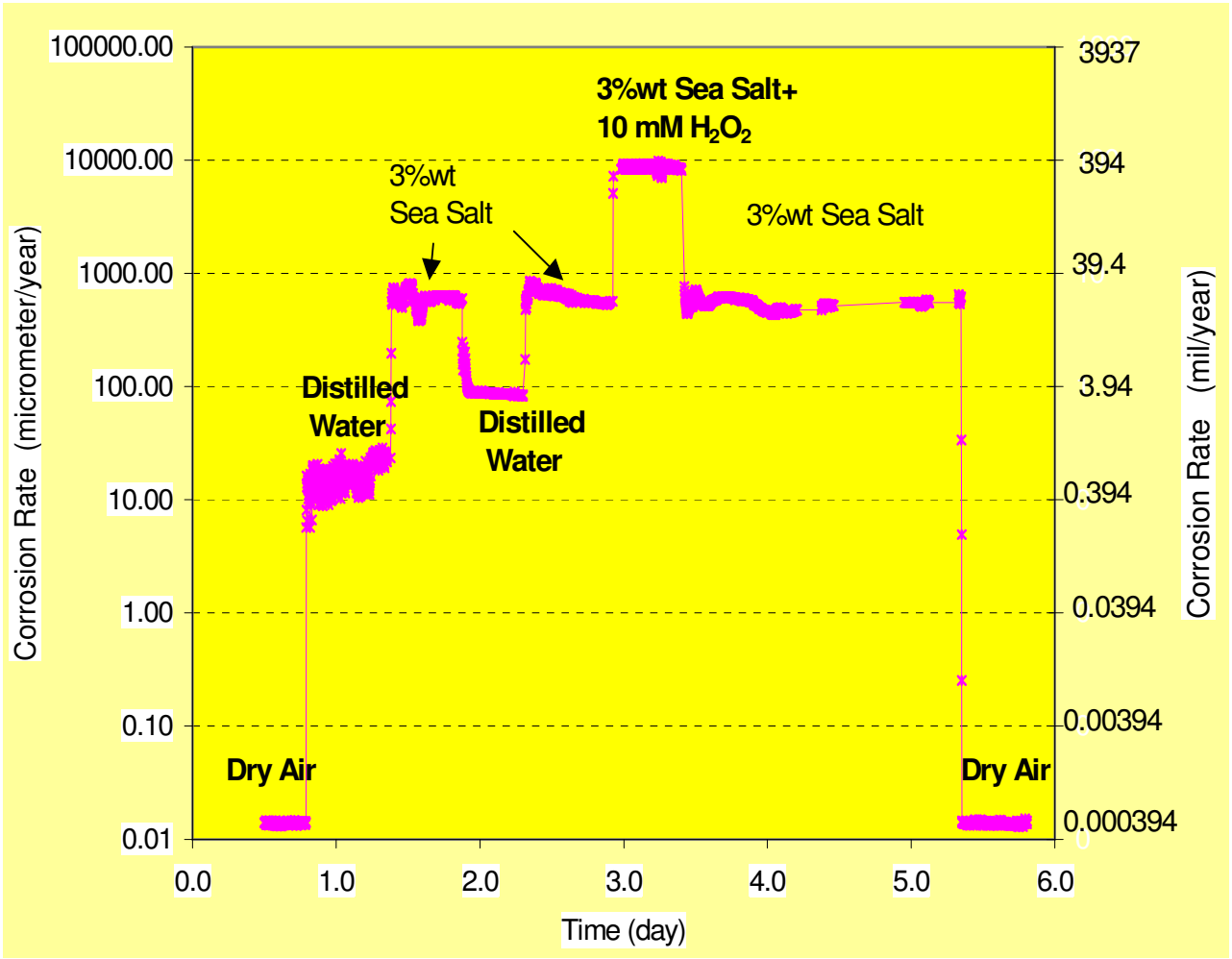

Figure 6. **Typical responses of a probe made of rebar carbon steel material to the changes of solution chemistry[12].**

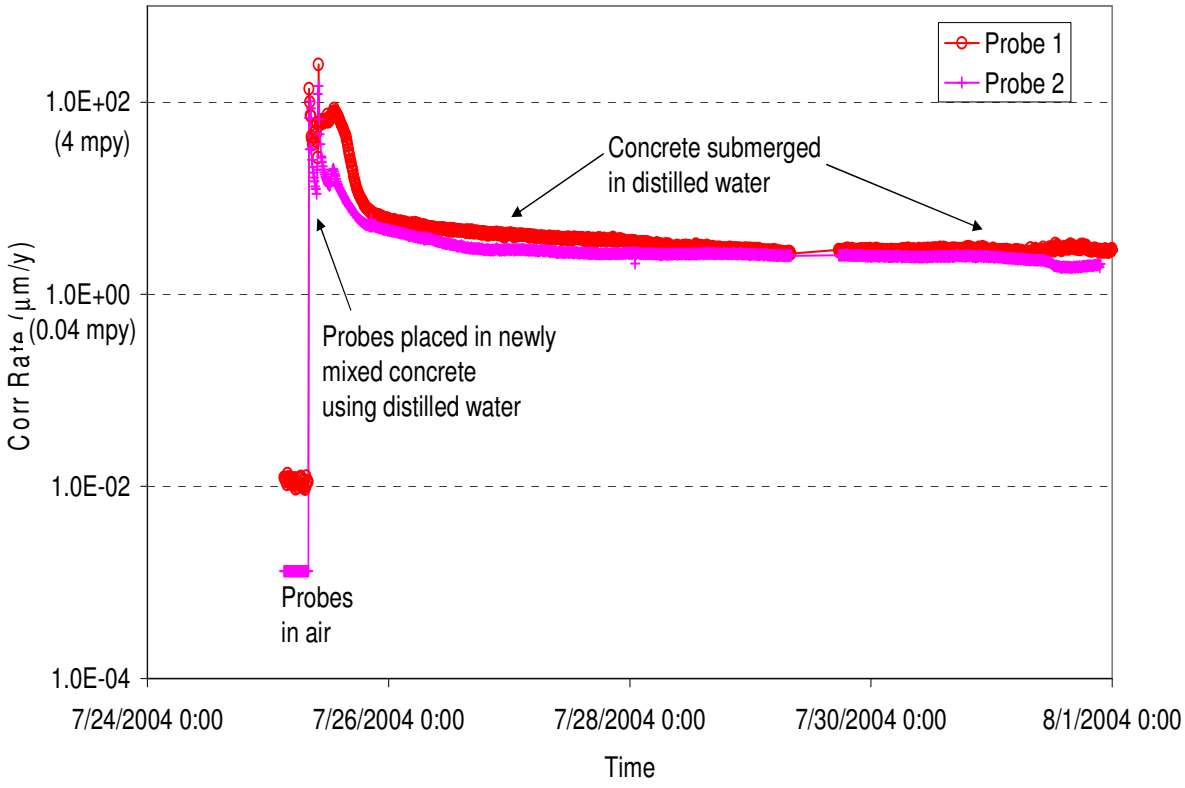

Figure 7. **Corrosion rates from two independent coupled multielectrode array probes made of rebar material in concrete submerged in distilled water.**

Note: **The corrosion rates in air were at or below the specified lower detection limit of the instrument (10 nm/year).**

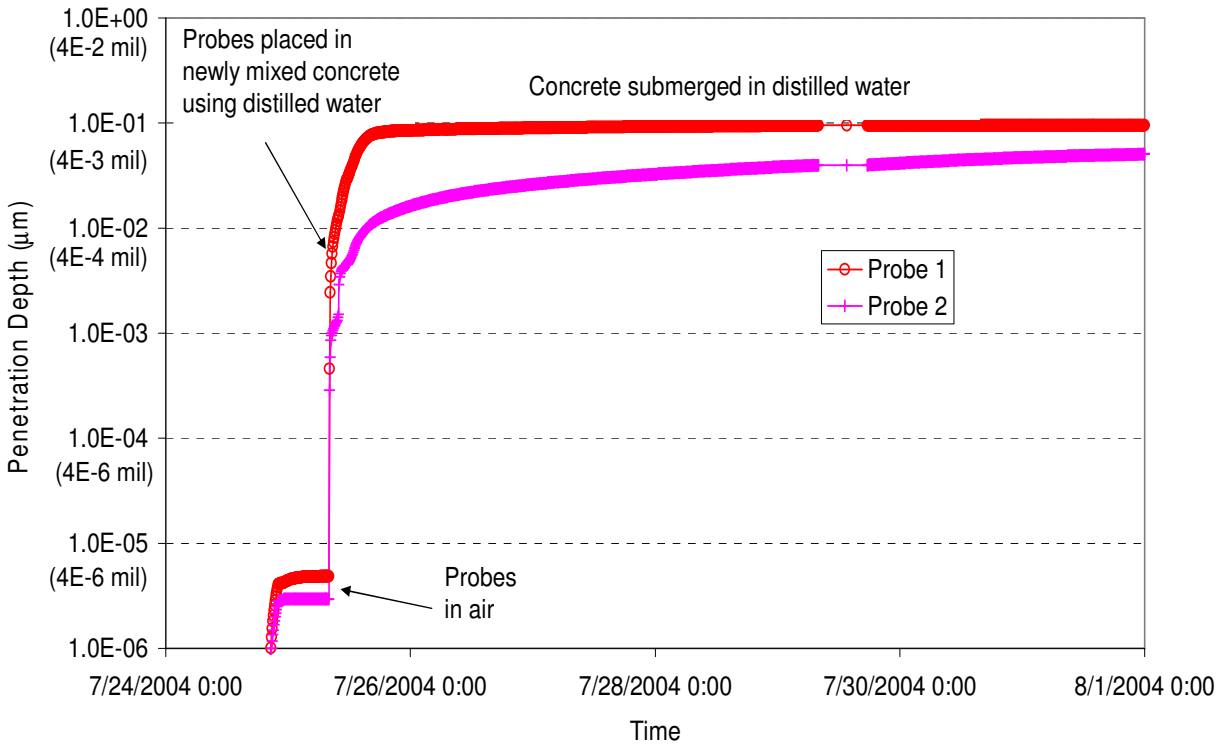

Figure 8. **Corrosion penetration depths calculated by the instrument software from the two independent coupled multielectrode array probes made of rebar material for the time period corresponding to *Figure 6.***

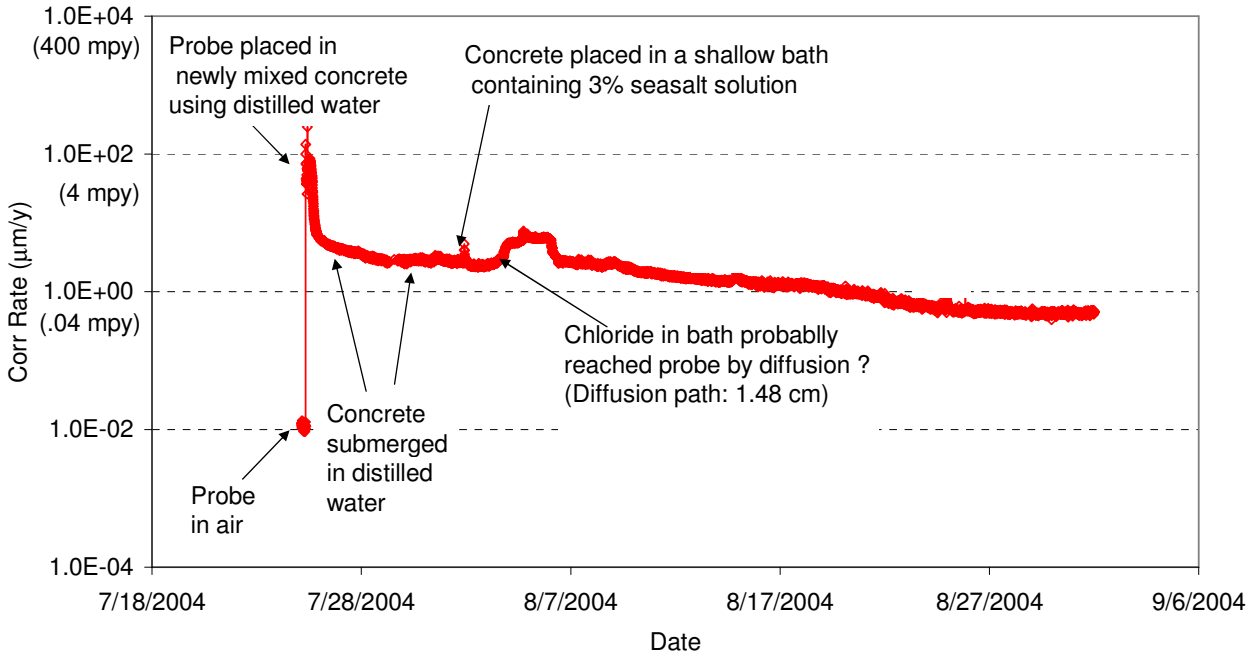

Figure 9. **Response of the non-uniform corrosion rate measured from the probe 1.48 cm from the concrete bottom surface to the immersion in simulated seawater. The increase in corrosion rate two days after the immersion in simulated seawater is probably due to the arrival of chloride to the probe by diffusion.**

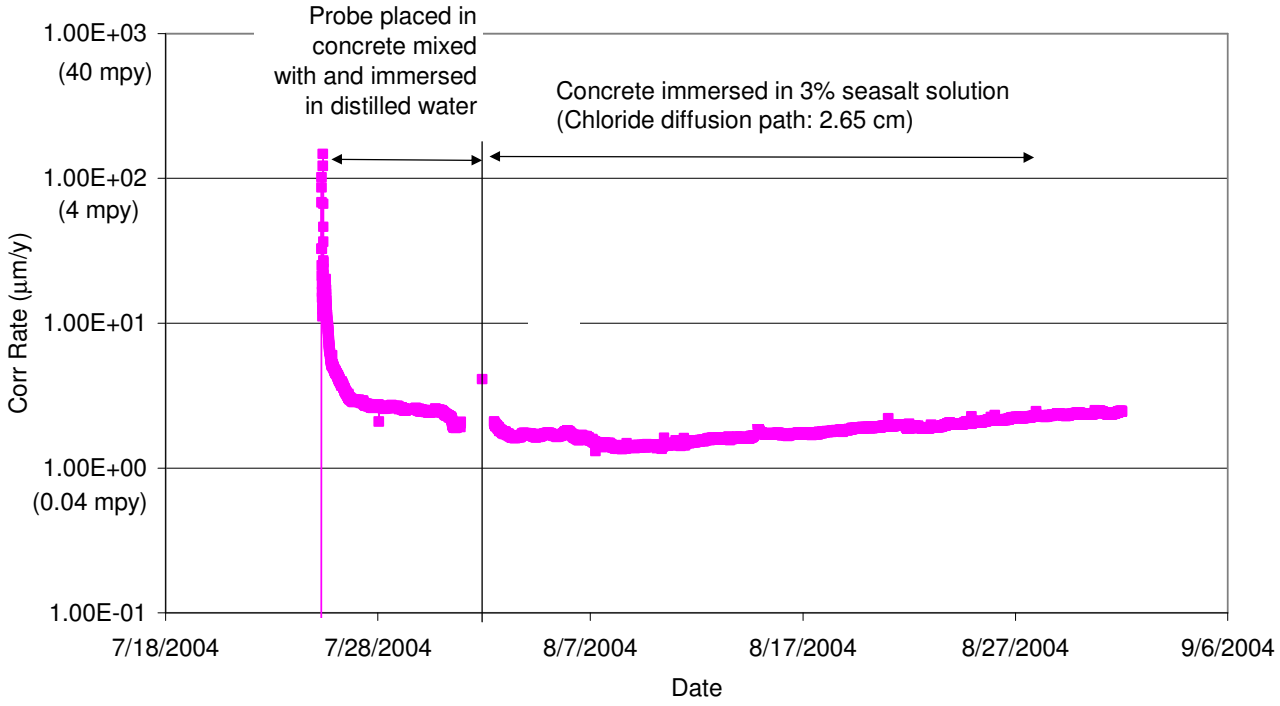

Figure 10. **Response of the non-uniform corrosion rate measured from the probe 2.65 cm from the concrete bottom surface to the immersion in simulated seawater. It is not clear if the slight increase 4 days after or the gradual increase 7 days after the immersion in the simulated seawater is due to the arrival of chloride to the probe.**

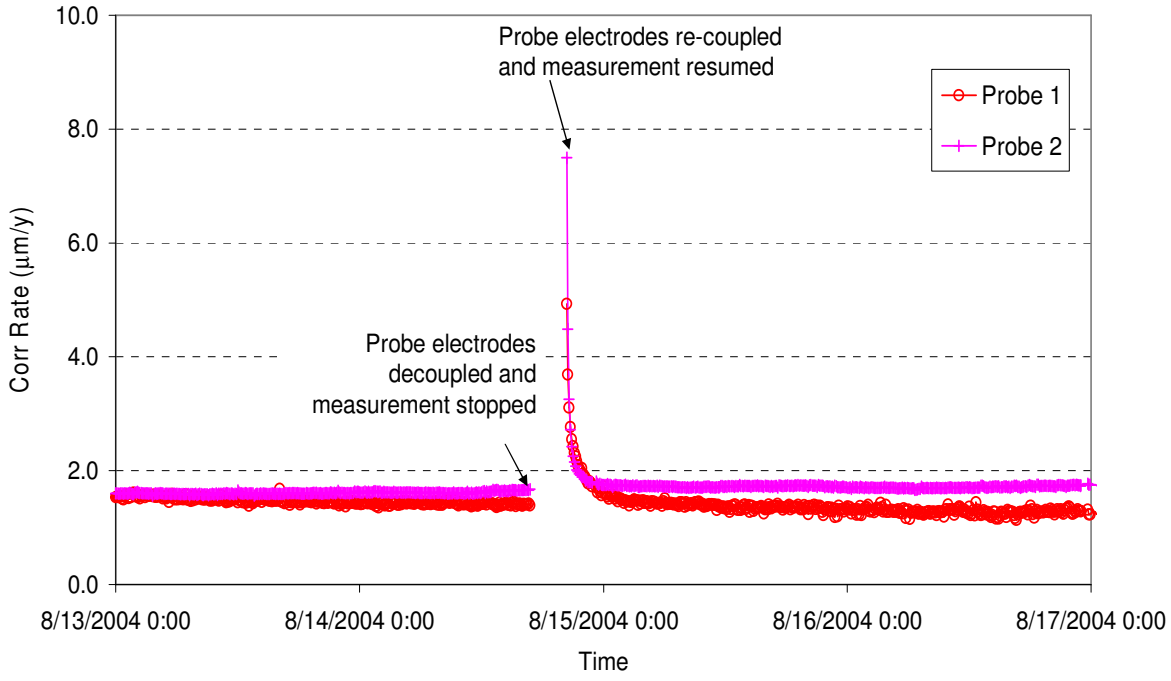

Figure 11. **Corrosion rates of rebar material measured from two coupled multielectrode array probes before and after the electrodes were decoupled (each electrode was disconnected from the coupling joint, see *Figure 1*).**

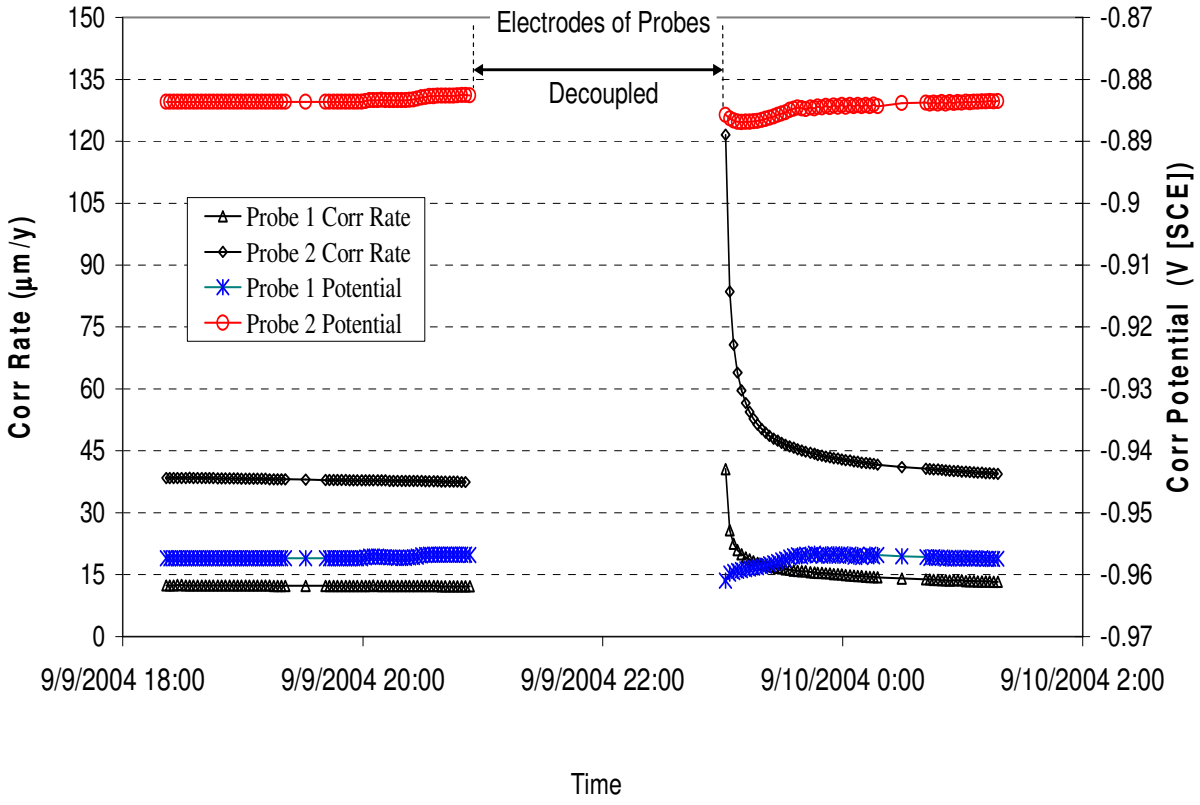

Figure 12. **Responses of the corrosion rates and corrosion potentials of two coupled multielectrode array probes to the decoupling of their electrodes.**

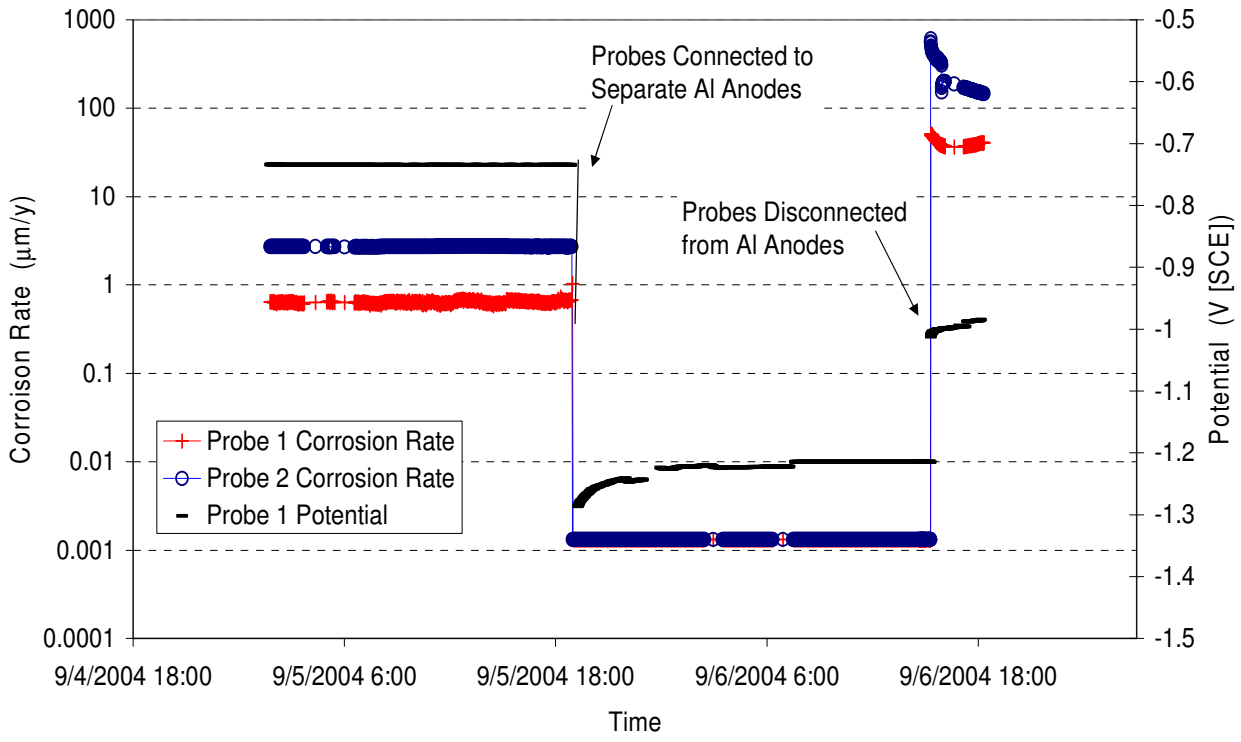

Figure 13. **Corrosion rates and potential of rebar material measured from two coupled multielectrode array probes before, during and after the probes were cathodically protected by sacrificial anodes.**